

MOL #65193

Identification of $5\alpha,6\alpha$ -epoxycholesterol as a Novel Modulator of LXR Activity

Thomas J. Berrodin[#], Qi Shen[#], Elaine M. Quinet, Matthew R. Yudt, Leonard P. Freedman¹ and Sunil Nagpal^{*2}

Women's Health & Musculoskeletal Biology, Wyeth Research, 500 Arcola Road, Collegeville, PA 19426, USA.

MOL #65193

RUNNING TITLE: Identification of a Novel LXR Modulator

Corresponding author: Sunil Nagpal, Merck Research Laboratories, 770 Sumneytown

Pike, West Point, PA 19846-0004, (Tel) 215-652-3281, (Fax) 215-993-0561,

sunil.nagpal@merck.com

Number of text pages: 29

Number of tables: 1

Number of figures: 10

Number of references: 39

Number of words in Abstract: 243

Number of words in Introduction: 670

Number of words in Discussion: 1470

Nonstandard abbreviations: ABCA1, ATP-binding cassette family transporter A1; ACACA, acetyl-Coenzyme A carboxylase alpha; Apo, apolipoprotein; CBP, CREB binding protein; DRIP, vitamin D receptor interacting protein; EC, epoxycholesterol; FASN, fatty acid synthase; Ivl, involucrin; KO, knockout; LBD, ligand binding domain; LDLR, low density lipoprotein receptor; LXR, liver X receptor; MFI, mean fluorescence intensity; NCoR, nuclear receptor corepressor; NRIP, nuclear receptor interacting protein; OHC, hydroxycholesterol; PLTP, phospholipid transfer protein; SCD, steroyl CoA desaturase; SMRT, silencing mediator of retinoic acid and thyroid hormone receptor; SRC, steroid receptor coactivator; SREBF, sterol response element binding factor; VDR, vitamin D receptor; wt, wild-type.

MOL #65193

ABSTRACT

The liver X receptors (LXR α and LXR β) are members of the nuclear receptor superfamily that function as key transcriptional regulators of a number of biological processes including cholesterol homeostasis, lipid metabolism and keratinocyte differentiation. Natural ligands that activate LXRs include oxysterol derivatives such as 25-hydroxycholesterol, 27-hydroxycholesterol, 22(R)-hydroxycholesterol, 20(S)-hydroxycholesterol and 24(S),25-epoxycholesterol. Related oxysterols, such as 5 α ,6 α -epoxycholesterol (5,6-EC) are present in a number of foods and have been shown to induce atherosclerosis in animal models. Intriguingly, these oxysterols have also been detected in atherosclerotic plaques. Using a variety of biochemical and cellular assays, we demonstrate that 5,6-EC is the first dietary modulator and an endogenous LXR ligand with cell- and gene-context dependent antagonist, agonist and inverse agonist activities. In a multiplexed LXR-cofactor peptide interaction assay, 5,6-EC induced the recruitment of a number of cofactor peptides onto both LXR α and LXR β , and showed an EC₅₀ of approximately 2 μ M in peptide recruitment. Further, 5,6-EC bound to LXR α in a radiolabeled ligand displacement assay (EC₅₀ = 76 nM), thus demonstrating it to be one of the most potent natural LXR α ligands known to date. Analysis of endogenous gene expression in various cell-based systems indicated the potential of 5,6-EC to antagonize LXR-mediated gene expression. Furthermore, it also induced the expression of some LXR-responsive genes in keratinocytes. These results clearly demonstrate that 5,6-EC is an LXR modulator that may play a role in the development of lipid disorders, such as atherosclerosis by antagonizing the agonistic action of endogenous LXR ligands.

MOL #65193

INTRODUCTION

Liver X receptors (LXR α /NR1H3 and LXR β /NR1H2) are oxysterol-dependent transcription factors that belong to the steroid/thyroid hormone nuclear receptor superfamily. LXR agonists induce the expression of genes involved in cholesterol efflux and transport, and decrease the expression of inflammatory mediators in macrophages and microglia (Chawla et al., 2001; Zelcer et al., 2007; Zelcer and Tontonoz, 2006). Therefore, LXR ligands have the potential to treat atherosclerosis and Alzheimer's disease (Joseph et al., 2002; Tontonoz and Mangelsdorf, 2003; Zelcer et al., 2007). In addition, LXR agonists display potent anti-inflammatory activities, and have shown therapeutic efficacy in murine models of dermatitis and rheumatoid arthritis (Chintalacharuvu et al., 2007; Fowler et al., 2003). Since the etiology of photoaging and chronological skin aging involves continuous cutaneous inflammation, LXR has also been identified and validated as a novel target for the prevention and treatment of skin aging (Chang et al., 2008). LXR ligands increase cholesterol efflux by inducing the expression of cholesterol binding (ApoE and ApoD) proteins and cholesterol transporters belonging to the ATP-binding cassette (ABC) family, namely, ABCA1, ABCG1, ABCG5 and ABCG8 (Zelcer and Tontonoz, 2006). In contrast, LXRs mediate their anti-inflammatory effects by antagonizing NF- κ B-mediated gene expression (Joseph et al., 2003). The mechanism underlying the anti-NF- κ B activity involves the recruitment of sumoylated LXR to the NF- κ B motif, which then prevents the degradation of associated N-CoR complexes (Ghisletti et al., 2007). A number of natural endogenous oxysterol ligands, namely, 24, 25-epoxycholesterol (24,25-EC), 22(R)-hydroxycholesterol (22-OHC), 20(S)-hydroxycholesterol (20-OHC), 25-hydroxycholesterol (25-OHC) and 27-

MOL #65193

hydroxycholesterol (27-OHC) that activate LXRs have been identified (Fu et al., 2001; Janowski et al., 1996; Lehmann et al., 1997).

Atherosclerosis is the most common cause of morbidity and mortality in the Western world. Atherosclerotic lesions as well as early fatty streaks contain cholesterol and its oxygenated derivatives, thus implicating oxysterols in the pathogenesis of atherosclerosis (Staprans et al., 1998; Staprans et al., 2003; Staprans et al., 2005; Staprans et al., 2000; Staprans et al., 2006). Oxysterols are also found in foam-cells or cholesterol-loaded macrophages that are the drivers of the initial phase of the disease (Hultén et al., 1996). Oxidation of cholesterol by autooxidation, lipid peroxidation or enzymatic oxidation gives rise to a number of oxysterols. In addition, processing of cholesterol-rich foods, such as meat, egg and dairy products and dried or stored fish also produces variable amounts of oxysterols that are consumed by humans. Oxysterols are postulated to be the key pro-atherogenic components since rabbits fed oxidized cholesterol show more severe focal arterial wall damage and atherosclerotic lesions than those fed non-oxidized cholesterol (Brown and Jessup, 1999; Staprans et al., 1998). Similarly, in a mouse model of atherosclerosis, oxysterols increased the lesion severity in the aorta (Staprans et al., 2000). The pathways and mechanisms by which oxysterols induce the pro-atherogenic effects are currently not understood. In addition, apart from cardiovascular disease and atherosclerotic lesions, oxysterols have been suspected to be involved in Alzheimer's disease, osteoporosis and age-related macular degeneration. 5 α ,6 α -epoxycholesterol (5,6-EC) is among the major oxysterols present in processed foods (Leonarduzzi et al., 2002), which is also detected in human plasma, chylomicrons and lipoproteins upon feeding oxysterol-rich diets (Björkhem et al., 1988; Gray et al.,

MOL #65193

1971; Staprans et al., 2005). In addition, serum concentration of 5,6-EC was higher in patients with hypercholesterolemia, and there appears to be a correlation between the serum levels of 5,6-EC and the degree of atherosclerosis (Björkhem et al., 1988; Gray et al., 1971). 5,6-EC is produced by autooxidation of cholesterol as well as endogenously by enzymatic reaction in the body involving cholesterol-5 α ,6 α -epoxidase (Smith and Johnson, 1989). Here, we demonstrate that 5,6-EC is the first dietary modulator of LXR activity, since it inhibited the agonist-mediated expression of various LXR target genes in multiple cell types and showed agonistic activity on the expression of some of the LXR-responsive genes in keratinocytes. Since LXR agonists have shown efficacy in vivo in models of atherosclerosis, Alzheimer's disease and inflammation, our results indicate that 5,6-EC may play a role in the development of lipid disorders by antagonizing the agonistic action of the endogenous LXR ligands.

MOL #65193

MATERIALS AND METHODS

Multiplex LXR-cofactor peptide interaction assay

Each unique fluorescently coded low capacity avidin modified Luminex bead (RADIX Biosolutions, Georgetown, TX) was incubated overnight with one of 39 biotinylated peptides (Anaspec, San Jose, CA) or biotin control at 12.5 μ M. The beads were washed twice with multiplex buffer (50mM TRIS pH 8.0, 50mM KCl) and incubated with 100 μ M D-biotin (Invitrogen, Carlsbad, CA) for 30min at room temperature to block any remaining unbound avidin sites. Following two additional washes, the beads were pooled and resuspended in multiplex buffer to make a 2X concentrated stock containing approximately 40,000 of each unique bead per milliliter. The assay was performed for two hours at room temperature in 100 μ l volume consisting of multiplex buffer, 10nM GST LXR α LBD protein (amino acids 207-447) or GST LXR β LBD protein (amino acids 243-461) (Invitrogen, Carlsbad, CA), 0.1% BSA, 2mM DTT, 0.8 μ g/ml anti-GST phycoerythrin antibody (Martek, Columbia, MD) and 1x peptide beads along with the test compounds. The plates were read on the Luminex (Austin, TX) instrument using standard settings with a minimum of 50 events quantified for each bead per well. Data were normalized by subtracting the background mean fluorescence intensity, determined with vehicle alone, from the mean fluorescence intensity obtained with each compound treatment.

Alphascreen Assay

The assays were performed for two hours at room temperature in 20 μ l volume containing 50mM TRIS pH 8.0, 50mM KCl, 0.1% BSA, 2mM DTT, 5nM GST LXR β LBD protein (amino acids 207-447) or GST LXR α LBD protein (amino acids 243-461) (Invitrogen,

MOL #65193

Carlsbad, CA), 5nM biotinylated cofactor peptide (Anaspec, San Jose, CA), 25 μ g/ml anti-GST acceptor and streptavidin donor AlphaScreen beads (PerkinElmer, Waltham, MA). The interaction between the receptor and cofactor peptide in the presence of test compounds were quantified using a PerkinElmer Envision plate reader with the standard AlphaScreen settings. Data were analyzed by a nonlinear regression model using SAS/Excel v1.03 software (SAS Institute, Cary, NC).

Mammalian Two-hybrid Assay

The ligand binding domains (LBD) of LXR α (amino acids 205-448) and LXR β (amino acids 219-462) were cloned into the pM GAL4-DBD vector (Clontech, Mountain View, CA). SRC-2 (amino acids 620-1121) was cloned into the pVP16 vector (Clontech, Mountain View, CA). For the GAL4UAS-luciferase reporter, 5 copies of the 17bp GALUAS sequence along with the E1b minimal TATA promoter were cloned into the pG5 basic luciferase vector (Promega, Madison, WI). Experiments were performed in COS-7 African green monkey kidney fibroblast-like cells (ATCC#CRL-1651) grown in phenol red-free Dulbecco's Modified Minimum Essential Medium (Gibco, Carlsbad, CA) supplemented with 10% charcoal/dextran-treated fetal bovine serum (Hyclone, Waltham, MA). The GAL4-LXR LBD fusion plamid, VP16 SRC-2 fusion plasmid and the GAL4UAS-luciferase reporter plasmid (50 ng/well each) were transfected for 16 h into COS-7 cells using Fugene6 (0.5 μ L/well) according to the manufacturer's protocol (Roche, Indianapolis, IN). Cells were treated with compounds for 20 hours and luciferase activity was measured using Cell Culture Lysis Buffer and Luciferase Reagent (Promega, Madison, WI) on a Victor2 luminometer (PerkinElmer, Waltham, MA). Data were

MOL #65193

analyzed by the nonlinear regression model using SAS/Excel v1.03 software (SAS Institute, Cary, NC).

LXR Binding Assay

LXR ligand binding domains with an N-terminal biotinylation tag expressed in *E.coli* were used for the LXR binding assays. For LXR α , amino acid residues 197-447 of human LXR α constituted the LDB. For LXR β , residues 154 – 461 of the human LXR β constituted the LDB. Cell extracts were made in 50mM Tris-HCl (pH = 7.4 at +4°C), 100 mM KCl, 8.6% glycerol, 0.1 mM PMSF, and 2 mM MTG. Tracer was 3H labeled T0901317 at 27 Ci/mmol (Amersham TRQ11134). Streptavidin-coated flash plates (SMP 103, NEN/Perkin Elmer) were washed with 100mM Tris- HCl (pH = 7.4 at +4°C), 100mM KCl, 8.6% glycerol, 0.1 mM PMSF, 2 mM MTG. Receptor extract was diluted so that 200 μ l of diluted extract gave a Bmax of around 4000 cpm. 200 μ l / well was added to the plate that was wrapped in Al-foil and incubated at +4°C over night. A dilution series of reference or test compound in 5nM tracer solution was made in Costar C3365 polypropylene microtiter plates. Assay buffer was 100mM Tris-HCl (pH = 7.4 at +4°C), 100mM KCl, 8.6% glycerol, 0.1 mM PMSF, 2 mM MTG, 0.2% CHAPS. LXR coated flash plates were washed three times with assay buffer without CHAPS, and residual buffer aspirated thoroughly. 200 μ l of test compound in 5 nM tracer was added to each well. Final concentrations of test compound ranged from 100 μ M to 50 pM, each concentration of test compound was analyzed in duplicate. Plates were wrapped in Al-foil and incubated over night at +4°C. Test compound / tracer mix was aspirated and plates washed once with assay buffer without CHAPS. Finally, residual liquid was aspirated and plates sealed according to instructions from the manufacturer. Radioactivity was

MOL #65193

measured in a Wallac Microbeta normalized for flashplates. Data were analyzed by the nonlinear regression model using XLfit software (IDBS, Guildford, Surrey UK).

Cell culture

Human hepatoma cell line Huh-7 and human lung adenocarcinoma epithelial cell line A549 were purchased from ATCC (Manassas, VA). Huh-7 cells were maintained in MEM/F12 : DMEM (3:1) with 10% FBS and A549 cells were cultured in low glucose DMEM with 10% FBS. In general, cells were seeded on day 0, treatment as designed was done on day 1, and cells were harvested on day 2 for RNA isolation using RNeasy column (Qiagen, Hilden, Germany). Gene expression profiles were analyzed using Taqman Low Density Array (TLDA) and individual Taqman gene assays (Applied Biosystems, Foster City, CA).

THP-1 cells (ATCC # TIB-202) were maintained in RPMI 1640 medium (Gibco, Carlsbad, Ca) containing 10% FBS, 2 mM L-glutamine, and 55 μ M β -Mercaptoethanol (BME). Confluent THP-1 cells were treated with 50-100 ng/ml phorbol 12,13-dibutyrate (Sigma, St.Louis, Mo) suspended in ethanol for three days to induce differentiation into adherent macrophages. LXR ligands dissolved in ethanol (EtOH) were added to differentiated cells for 18 hrs, then total cellular RNA was isolated using a PrepStation 6100 (Applied Biosystems, Foster City, Ca) according to the manufacturer's recommendations. RNA concentrations measured with RiboGreen assay, #R-11490 (Molecular Probes, Eugene, OR) and hABCA1 mRNA quantified by real-time PCR analysis as previously described (Quinet et al., 2004). For antagonism studies, the T0901317 agonist was dosed at its EC₅₀ concentration.

LXR β WT and KO skin cell preparations

MOL #65193

LXR- β KO mice were obtained from Deltagen (San Carlos, CA) in the 129 strain and backcrossed for seven generations into black C57BL/6J mice. LXR- β KO was accomplished using LXR- β gene sequence deletion from base 226 to 395 by using a homologous recombination vector (Deltagen, San Carlos, CA). Skins from newborn mice (2-3 days old) were isolated and floated on 2.5 mg/ml dispase (Invitrogen/Gibco, Carlsbad, CA) overnight at 4°C and separated into epidermal and dermal layers using small forceps. The epidermal and dermal layers were minced and subjected to several differential centrifugations, fractionations and filtrations as previously described (Zheng et al., 2005). These cells were then cultured in Eagle's minimal essential medium containing fetal bovine serum (8 %) in 24-well culture plates (day 0). Cells were treated as described on day 2, followed by isolation and purification of RNA on day 3 using RNeasy column.

Custom-designed TLDAs and quantitative RT-PCR

The RNA obtained from the compound treated cells were used in custom-designed TLDAs or individual Taqman assays (Applied Biosystems, Foster City, CA) as per vendor's protocols using ABI 7900HT real-time PCR machine. The level of expression was calculated based on the PCR cycle number (Ct), and the relative gene expression level was determined using $\Delta\Delta C_t$ method as described elsewhere. One TLDA was designed with oligo probes and primer pairs for *Ivl* (Mm00515219_s1), *Abca1* (Mm00442646_m1), *ApoE* (Mm00437573_m1), *Scd1* (Mm00772290_m1), *Cyp27a1* (Mm00470430_m1), *ABCA1* (Hs00194045_m1), *ACACA* (Hs00167385_m1), *FASN* (Hs00188012_m1), *LDLR* (Hs00181192_m1), *PLTP* (Hs00272126_m1), *SLC2A4*

MOL #65193

(Hs00168966_m1), SREBF1 (Hs00231674_m1), ABCG1 (Hs00245154_m1) and SCD1
(Hs00748952_s1).

MOL #65193

RESULTS

5,6-EC recruits cofactor peptides to LXR LBD proteins

Nuclear receptors (NRs), including LXRs, activate gene expression by ligand-dependent interaction with coactivators that act by modifying chromatin structure and mediating interaction with components of the basal transcription machinery. It has been proposed that NR modulators function in a tissue-selective manner by inducing unique receptor conformations that lead to differential recruitment of coactivators. These coactivators are specifically recruited to NRs via their LXXLL modules, and small peptides containing LXXLL motifs are sufficient to bind to the receptor in a ligand-dependent manner (Heery et al., 1997; Savkur et al., 2004). Since various oxysterols have been identified as LXR ligands, we decided to examine if 5,6-EC is also an LXR ligand by analyzing the recruitment of 39 cofactor peptides (Berrodin et al., 2009) to LXR α and β ligand binding domains (LBDs) in a biochemical microsphere-based multiplex NR-cofactor interaction assay (Berrodin et al., 2009; Iannone et al., 2004). The sequences of cofactor peptides used herein are shown in Table 1. The structure of 5,6-EC as well as the structures of known natural and synthetic LXR ligands is shown (Fig. 1). A saturating concentration (10 μ M) of 5,6-EC was used to compare its cofactor recruitment profile with that of other known synthetic and natural oxysterol LXR ligands. The ligand-dependent recruitment of cofactor peptides to the LXR α or β LBDs is expressed as mean fluorescence intensity (MFI) units, which is directly proportional to the affinity of the peptides to the receptor LBD protein. As shown in fig. 1A, the synthetic LXR ligand T0901317 (Schultz et al., 2000) showed robust interaction with SRC-1II, SRC-1IV, SRC-2II, SRC2-III, SRC-3, DRIP205 II, PGC-1 α , CBP I, p300 I and various NRIP1 peptides.

MOL #65193

However, a number of cofactor peptides did not show any binding to LXR α -LBD, and the most potent natural endogenous ligand, 24,25-EC was less efficacious than T0901317 in recruiting most of the peptides to the receptor LBD (Fig. 2A). Notably, T0901317 and 24,25-EC induced distinct receptor conformations since the former mediated the dissociation of LXR α -LBD-SMRT II peptide interaction, whereas, the later induced the recruitment of the corepressor peptide to the LXR α LBD protein (Fig.2A). 22-OHC was approximately 50% less efficacious than 24,25-EC but still showed interaction with similar set of peptides. Interestingly, 5,6-EC was less efficacious than T0901317 and 24,25-EC but exhibited efficacy similar to that of 22-OHC on SRC-2 III, SRC-3 III, DRIP 205 II and NRIP1 VI peptides (Fig. 2A). However, unlike the other natural and synthetic LXR ligands (except 25-OHC), 5,6-EC did not mediate LXR α -LBD interaction with CBP I, p300 I, SMRT II and NRIP1 II peptides. The interaction profile revealed that 5,6-EC engendered a conformational change in the LXR α -LBD, which was different from that mediated by the T0901317 and other oxysterol natural ligands. 25-OHC was the least efficacious of all in this assay (Fig. 2A).

In interaction assay with LXR β -LBD, T0901317 and 24,25-OHC showed similar profiles and were equally efficacious in mediating interaction with similar set of peptides (Fig. 2B). 22-OHC and 25-OHC showed similar cofactor peptide interaction patterns (Fig. 2B). Interestingly, 5,6-EC exhibited distinct cofactor peptide interaction profile and mediated the recruitment of only three cofactor peptides, namely SRC-2 II, SRC-3 III and NRIP1 VI (Fig. 2B). In addition, 5,6-EC was the least efficacious ligand on LXR β -LBD (Fig. 2B). Furthermore, all the other ligands except 5,6-EC showed the dissociation of SMRTII corepressor peptide from the LXR β -LBD protein. These results indicate that

MOL #65193

5,6-EC induces LXR β -LBD conformation, which is different from that engendered by the other ligands.

In a biochemical Alphascreen-based dose-dependent LXR α -SRC-2 III recruitment assay, 5,6-EC was nearly as efficacious as 24,25-EC and showed EC₅₀ value of 1.7 μ M. T0901317, 24,25-EC, 22-OHC and 25-OHC showed EC₅₀ values of 0.32, 0.87, 2.3 and 22 μ M, respectively (Fig. 3A). In LXR β -SRC-2 III interaction assay, T0901317, 5,6-EC, 24,25-EC, 22-OHC and 25-OHC showed EC₅₀ values of 0.03, 1.3, 0.18, 0.57 and 3.4 μ M, respectively (Fig. 3B). Similarly, in LXR-SRC-3 III cofactor recruitment assays, 5,6-EC showed EC₅₀ values of 1.9 and 2.8 μ M for LXR α and LXR β , respectively (Fig. 3C and D). In LXR α -SRC-3 III recruitment assay, 5,6-EC was 50% less efficacious than T0901317, whereas it showed efficacy and potency equivalent to that of 20-OHC and 22R-OHC (Fig. 3C). These results clearly demonstrate that 5,6-EC shows single digit μ M EC₅₀ values in cofactor-dependent LXR α and β ligand-sensing assays and it exhibits greater efficacy with LXR α than LXR β LBD when compared to T0901317.

5,6-EC binds to LXR α and mediates cofactor recruitment in cells

A ligand competition assay was employed to assess the direct binding of 5,6-EC using recombinant human LXR α and β LBD proteins and ³H-labeled T0901317 as a tracer (Hu et al., 2006). Sigmoidal competition curve was obtained for the binding of 5,6-EC to LXR α LBD but no competition of ³H-labeled T0901317 was observed in LXR β LBD-based binding assays. 5,6-EC showed IC₅₀ value of 76 nM for LXR α in the ligand competition assay (Fig. 4A). However, it failed to significantly displace the radiolabeled synthetic LXR agonist in LXR β binding assay (Fig. 4A). In contrast, 24-25-EC showed

MOL #65193

IC₅₀ values of 370 nM and 390 nM, respectively for LXR α and LXR β LBDs (Fig. 4B). These results indicate that 5,6-EC binds directly to the LXR α -LBD, and exhibits 5-fold more potency than 24, 25-EC. In addition, 5,6-EC is unable to displace the radiolabeled T0901317 from the LXR β -LBD protein.

To determine whether the binding of 5,6-EC to LXR recruits coactivator SRC-2 in a cell-based system, a mammalian two-hybrid system with Gal4-LXR α or β and VP16-SRC-2 expression vectors was employed. 5,6-EC showed a dose-dependent recruitment of VP16-SRC-2 to LXR α but not LXR β -LBD (Fig. 5). In LXR α -SRC-2 mammalian two-hybrid assay, 5,6-EC showed partial agonism (when compared to T0901317 and 24,25-EC), and was also the least potent ligand among all the LXR agonists tested. Moreover, 5,6-EC showed 75% and 67%, respectively less efficacy than T0901317 and 24,25-EC. In contrast, 5,6-EC failed to mediate LXR β -LBD-SRC2 interaction, whereas all the other ligands tested were active. T0901317 and 24,25-EC were equipotent in mediating LXR β -SRC-2 interaction (Fig. 5). These results indicate that 5,6-EC may function as an antagonist and inhibit agonist-mediated expression of the LXR-responsive genes.

5,6-EC is a modulator of LXR-mediated gene expression in primary murine keratinocytes

Multiplex LXR cofactor interaction, AlphaScreen and binding assays indicated that 5,6-EC could bind to LXRs. However, in the absence of VP16-SRC-2, it did not induce Gal4-LXR α / β -mediated activation of a Gal4-responsive reporter (data not shown). Therefore, we next examined if 5,6-EC could act as an antagonist, and analyzed its effect on the expression of known LXR-responsive genes in primary mouse

MOL #65193

keratinocytes. In these cells, 5,6-EC did not induce the expression of *Abca1* or *involucrin* (*Ivl*) but effectively antagonized the 24,25-EC-mediated expression of these genes. The 24,25-EC agonism as well as 5,6-EC antagonism effects were not observed in *LXR β* KO keratinocytes (Fig. 6A and B). We also analyzed the effect of 5,6-EC on *Apo e*, *Scd1* and *Cyp27a1*, which are also known *LXR*-responsive genes. 5,6-EC inhibited the basal level expression, while T0901317 and 24,25-EC induced the expression of *Apo e*. 5,6-EC completely antagonized the T0901317 and 24,25-EC-dependent expression in wild-type (wt) keratinocytes. The agonist effects of T0901317 and 24,25-EC as well as the antagonist effects of 5,6-EC were not observed in *LXR β* KO keratinocytes, thus demonstrating the specificity of the *LXR* agonist as well as that of 5,6-EC action (Fig. 7A). In contrast to its effect on *Abca1*, *Ivl* and *Apo e*, 5,6-EC augmented the expression of *Scd1* in wt but not in *LXR β* KO keratinocytes (Fig. 7B). *Scd1* expression was also induced by T0901317 but not by 24,25-EC in keratinocytes. Note that 5,6-EC was a partial agonist on keratinocyte *Scd1* expression when compared to T0901317 (Fig. 7B). In contrast to other responsive genes, we show that *Cyp27a1* expression was induced by 5,6-EC and not by other classical *LXR* ligands in wild-type cells but not in *LXR β* KO keratinocytes (Fig. 7C). These results indicate that in keratinocytes, 5,6-EC is a gene-selective modulator of *LXR* action since it could act as an inverse agonist, partial agonist, full agonist or an antagonist of *LXR*-mediated gene expression.

5,6-EC is an antagonist of *LXR* agonist-mediated gene expression in Huh-7 and A549 cells

We also examined the effect of 5,6-EC on the expression of classical *LXR*-responsive genes in Huh-7 (human hepatocarcinoma) and A549 (human lung carcinoma)

MOL #65193

cells in agonist and antagonist modes in the presence of the synthetic LXR agonist T0901317. 5,6-EC decreased the basal level expression of SLC2A4 and FASN, and antagonized the T0901317-mediated expression of these genes in Huh-7 cells (Fig. 8A and C). On the other hand, 5,6-EC did not significantly affect the basal level expression of SREBF1, PLTP, ACACA and LDLR (Fig. 8B and D-F). However, it significantly antagonized the T0901317-mediated expression of these genes (Fig. 8 A-F). Similarly, 5,6-EC was an antagonist in A549 cells, since it inhibited the T0901317-induced expression of ABCA1, ABCG1, ACACA, FASN, SCD1 and LDLR (Fig. 9 A-F). Note that 5,6-EC induced the expression of SCD1 in keratinocytes (Fig. 6C) but not in A549 (Fig 9E), thus indicating that 5,6-EC is a cell-context dependent modulator of LXR-mediated gene expression.

5,6-EC is a partial agonist in differentiated THP-1 macrophages

In differentiated THP-1 macrophages, T0901317 and 24,25-EC induced the expression of ABCA1 in a dose-dependent manner with EC₅₀ values of 0.024 and 7.7 μM, respectively (Fig. 10A). In contrast, 5,6-EC was a partial agonist on ABCA1 gene expression in THP-1 cells, and it showed only 23% efficacy (relative to T0901317) when tested at the maximum concentration of 30 μM (Fig. 10A). Interestingly, unlike in keratinocytes (Fig. 6A), 5,6-EC did not significantly affect T-0901317-induced expression of ABCA1 gene in THP-1 macrophages, thus highlighting the cell-context dependent antagonism activity of 5,6-EC (Fig. 10B). Accordingly, 5,6-EC would not be expected to inhibit T0901317-mediated cholesterol efflux in macrophages. Note that 5,6-EC induced ABCA1 expression only in THP-1 macrophages (Fig. 10A) but not in

MOL #65193

keratinocytes, Huh-7 or A549 cells, further indicating the cell-context dependent activity of 5,6-EC.

MOL #65193

DISCUSSION

This manuscript describes for the first time that 5,6-EC is a dietary and endogenous modulator of LXR activity. Oxidized cholesterol has been implicated in the pathophysiology of atherosclerosis (Hu et al., 2006; Leonarduzzi et al., 2002; Staprans et al., 1998; Staprans et al., 2003; Staprans et al., 2005; Staprans et al., 2000; Vine et al., 1998). However, the mechanism by which oxidized cholesterol species might provoke oxidative insult is not understood. Cholesterol undergoes rapid autooxidation, peroxidation and photooxidation, giving rise to various oxidized derivatives, namely, 5,6-EC, 7-ketocholesterol and 25-OHC, which have been identified in human plasma (Brown and Jessup, 1999; Gray et al., 1971). Various oxidized cholesterol derivatives have been detected in lipids extracted from atheromatous aortic lesions (Brown and Jessup, 1999) and oxidation products of cholesterol are known to increase the severity of fatty streak lesions in rabbit and mouse models of atherosclerosis (Staprans et al., 1998; Staprans et al., 2000). Animal food products (milk, eggs, meat and their products) are the major source of cholesterol in our diet. Processing of foods and oils involving high temperature and prolonged storage has been reported to induce the oxidation of cholesterol. Other chemical species such as hydroxyl radicals, ozone, oxygen cations, singlet oxygen, superoxide and peroxides could also aid in the autooxidation of cholesterol (Kumar and Singhal, 1991). Therefore, 5,6-EC and other oxygenated cholesterol derivatives could be generated in the food products before consumption and could also result from the oxidation of endogenous cholesterol. In addition, cholesterol loading of human monocyte-derived macrophages has shown the production of 5,6-EC in quantities comparable to that of 27-OHC (Fu et al., 2001). Although there is no direct proof linking

MOL #65193

oxidized cholesterol to atherosclerosis in humans, a plethora of *in vitro* and *in vivo* studies have highlighted the atherogenic potential of diets rich in oxidized cholesterol (Gray et al., 1971; Kumar and Singhal, 1991; Staprans et al., 1998; Staprans et al., 2000). In fact in humans, dietary 5,6-EC after a single meal is absorbed and incorporated into the pool of oxidized lipids in chylomicrons and endogenous (VLDL, LDL and HDL) lipoproteins. Furthermore, after a single dose, 5,6-EC remained in circulation with lipoproteins for 72 hours, and an increase in oxidized cholesterol content in LDL is associated with increased susceptibility of these particles to undergo further oxidation, thus resulting in a larger pool of oxidized cholesterol derivatives (Staprans et al., 2003). These observations indicate that oxidized cholesterol derivatives, including 5,6-EC may contribute to the pathogenesis of atherosclerosis.

Here, we show that 5,6-EC (Fig. 1) is an LXR modulator since it mediated the interaction of various coactivator peptides to LXR α and β LBD proteins (Fig. 2), showed dose-dependent interaction of coactivator peptides with the LXR in biochemical assays (Fig. 3), exhibited binding to LXR α -LBD in a ligand competition assay (Fig. 4), and modulated the expression of various LXR-responsive genes in keratinocyte, liver and lung cells (Figs. 6-9). 5,6-EC inhibited the binding of ^3H -labeled T0901317 to LXR α with an EC_{50} value of 76 nM, thus indicating it to be a potent LXR α ligand (Fig. 4). However, it failed to show the displacement of the radiolabeled ligand in the presence of LXR β LBD in the ligand competition assay (Fig. 4). The interaction of cofactor peptides to LXR α and β LBD proteins (Figs. 2 and 3), and the LXR β -dependent modulation of gene expression in murine keratinocytes (Fig. 6) suggest 5,6-EC to be a bonafide ligand of LXR α and β isoforms. The differential action of 5,6-EC in displacing ^3H -T0901317

MOL #65193

from the LXR LBDs could result from high $K(\text{on})$ and low $K(\text{off})$ rates of the radiolabeled synthetic ligand on the LXR β subtype. This phenomenon has been observed in the case of vitamin D receptor (VDR) ligands, where potent VDR agonists did not displace radiolabeled 1,25-dihydroxyvitamin D₃ because of its high $K(\text{on})$ and low $K(\text{off})$ for the receptor (Boehm et al., 1999; Ma et al., 2006). Our biochemical AlphaScreen-based assays using purified LXR α and β LBD proteins and synthetic cofactor LXXLL motif peptide (SRC-2 NR box III) clearly demonstrate that 5,6-EC is bonafide ligand of both LXR α and β subtypes, with at least a single digit μM potency (Fig. 3). 5,6-EC showed comparable efficacy and potency to oxysterol natural known LXR ligands in LXR α -SRC-2 and SRC-3 peptide interaction assays and it also mediated LXR β -LBD interaction with SRC-2/SRC-3, albeit with potency lower than that of 24,25-EC, 22(R)-OHC and 20(S)-OHC (Fig. 3). However, it showed significantly better potency than 25-OHC in mediating the interaction of LXXLL peptides onto LXR α and β LBDs (Fig. 3). Taken together, these results clearly indicate that 5,6-EC is a novel ligand for both LXR subtypes.

Herein, our results demonstrate that 5,6-EC is a novel LXR modulator with cell- and gene-context dependent activities (Figs. 5-8). It has been postulated that the tissue- and gene-selective activities of nuclear receptor modulators are due to their abilities to induce distinct conformational changes in the LBD of the receptor, which may result in differential recruitment of cofactors required for the regulation of target gene expression. In the multiplex cofactor peptide interaction assays, 5,6-EC showed distinct profiles of LXR α and LXR β LBD - peptide interactions that were different from that obtained with T0901317 and known oxysterol LXR ligands (Fig. 1). These results clearly indicate that

MOL #65193

5,6-EC induces LXR-LBD conformations that are different from that engendered by T0901317, 22-OHC, 25-OHC and 24,25-OHC. The ligand-mediated differential conformations of the receptor may result in differential cofactor recruitment, leading to cell-context dependent activity as observed with non-calcemic vitamin D receptor modulators (Ma et al., 2006). Furthermore, enhanceosome level interaction between LXR with other interacting transcription factors in addition to differential cofactor recruitment may also explain the cell/gene-context dependent activation of gene expression. Such an interaction and its effect on lineage-specific transcription have been described for ER α with FOXA1 (Lupien et al., 2008).

LXR is a key regulator of cholesterol homeostasis. Agonist ligands of LXR induce the expression of genes involved in cholesterol efflux and transport (ABCA1, ABCG1, ABCG5, ABCG8, Apo E and Apo D), and also decrease the expression of key mediators of inflammation (Chawla et al., 2001; Zelcer and Tontonoz, 2006). These activities are the basis of the efficacious effects of LXR ligands in murine model of atherosclerosis and Alzheimer's disease (Joseph et al., 2002; Tontonoz and Mangelsdorf, 2003; Zelcer et al., 2007). LXR ligand also display potent anti-inflammatory activities in keratinocyte, fibroblast and immune cell systems, and as a result show efficacy in murine models of atopic and contact dermatitis, rheumatoid arthritis and photoaging (Chang et al., 2008; Chintalacharuvu et al., 2007; Fowler et al., 2003). In addition, LXR ligands are potent keratinocyte differentiation agents and are also involved in the maintenance of epidermal barrier function by regulating lipid production in keratinocytes (Chang et al., 2008; Kömüves et al., 2002; Man et al., 2006). Therefore, LXR as a target has wide-ranging therapeutic potential in atherosclerosis, arthritis, dermatitis, psoriasis and skin

MOL #65193

aging. The discovery reported herein of a natural dietary and endogenous LXR modulator that antagonizes the action of key genes involved in cholesterol transport, lipogenesis and keratinocyte differentiation is significant. Our results provide a mechanism by which oxidized cholesterol derivatives may induce the formation and progression of atherosclerotic lesions. To the best of our knowledge 5,6-EC is the first food processing related modulator of any nuclear receptor. Our results also may explain the underlying reason for the high incidence of atherosclerosis and cardiovascular events observed in Indian/Asian immigrant population in Western countries, which could not be explained by major predisposing factors of hypertension, smoking, intake of red meat, serum cholesterol and alcohol consumption. One of the risk factors unique to this population may be the ingestion of exceptionally high quantities of oxidized cholesterol (Jacobson, 1987). For example it has been reported that clarified butter or ghee used as cooking oil medium may be a causative factor for the high incidence of cardiovascular diseases in this population, since it contains a number of cholesterol oxidation products including 5,6-EC (Jacobson, 1987). Therefore, the identification of 5,6-EC as an antagonist of LXR-mediated gene expression provides a molecular level explanation of the above-mentioned epidemiological observations. Although 5,6-EC did not antagonize T0901317 action on ABCA1 expression in THP-1 macrophages (Fig. 10B), we can not rule out the possibility that it may antagonize the action of endogenous weaker LXR oxysterol ligands in vivo.

In summary, we have identified 5,6-EC as the first novel dietary and endogenous modulator of LXR activity. 5,6-EC is also the most potent natural ligand known for LXR α subtype as assessed by ligand competition binding assay. It mainly functions as an

MOL #65193

antagonist on a number of classical LXR-responsive genes, but in addition, shows agonist and inverse agonist activities in a cell- and gene-context dependent manner. It will be an important tool in further elucidating the physiological role of LXRs and oxysterols in cholesterol/lipid homeostasis, atherosclerosis, inflammation, keratinocyte differentiation and epidermal barrier formation.

Acknowledgements

We thank R. Bernotas and Annika Goos-Nilsson for the ligand binding assays, and Harold Selnick for help in preparing figure 1. We are also thankful to Wei Wang for providing us with wt and LXR β KO mouse keratinocytes.

MOL #65193

REFERENCES

- Berrodin TJ, Chang KC, Komm BS, Freedman LP and Nagpal S (2009) Differential biochemical and cellular actions of Premarin estrogens: distinct pharmacology of bazedoxifene-conjugated estrogens combination. *Mol. Endocrinol.* 23:74-85.
- Björkhem I, Breuer O, Angelin B and Wikström SA (1988) Assay of unesterified cholesterol-5,6-epoxide in human serum by isotope dilution mass spectrometry. Levels in the healthy state and in hyperlipoproteinemia. *J. Lipid Res.* 29:1031-1038.
- Boehm MF, Fitzgerald P, Zou A, Elgort MG, Bischoff ED, Mere L, Mais DL, Bissonnette RP, Heyman RA, Nadzan AM, Reichman M and Allegretto EA (1999) Novel nonsecosteroidal vitamin D mimics exert VDR-modulating activities with less calcium mobilization than 1,25-dihydroxyvitamin D3. *Chemistry & Biology* 6:265-275.
- Brown AJ and Jessup W (1999) Oxysterols and atherosclerosis. *Atherosclerosis* 142:1-28.
- Chang KC, Shen Q, Oh IG, Jelinsky SA, Jenkins SF, Wang W, Wang Y, LaCava M, Yudt MR, Thompson CC, Freedman LP, Chung JH and Nagpal S (2008) Liver X receptor is a therapeutic target for photoaging and chronological skin aging. *Mol. Endocrinol.* 22:2407-2419.
- Chawla A, Repa JJ, Evans RM and Mangelsdorf DJ (2001) Nuclear receptors and lipid physiology: opening the X-files. *Science* 294:1866-1870.
- Chintalacharuvu SR, Sandusky GE, Burris TP, Burmer GC and Nagpal S (2007) Liver X receptor is a therapeutic target in collagen-induced arthritis. *Arthritis Rheum.* 56:1365-1367.
- Fowler AJ, Sheu MY, Schmith M, Kao J, Fluhr JW, Rhein L, Collins JL, Willson TL, Mangelsdorf DJ, Elias PM and Feingold KR (2003) Liver X receptor activators display anti-inflammatory activity in irritant and allergic contact dermatitis models: liver-X-receptor-specific inhibition of inflammation and primary cytokine production. *J. Invest. Dermatol.* 120:246-255.
- Fu X, Menke JG, Chen Y, Zhou G, MacNaul KL, Wright SD, Sparrow CP and Lund EG (2001) 27-hydroxycholesterol is an endogenous ligand for liver X receptor in cholesterol-loaded cells. *J. Biol. Chem.* 276:38378-38387.
- Ghisletti S, Huang W, Ogawa S, Pascual G, Lin ME, Willson TM, Rosenfeld MG and Glass CK (2007) Parallel SUMOylation-dependent pathways mediate gene- and signal-specific transrepression by LXRs and PPARgamma. *Mol. Cell* 25:57-70.
- Gray MF, Lawrie TD and Brooks CJ (1971) Isolation and identification of cholesterol -oxide and other minor sterols in human serum. *Lipids* 6:836-843.
- Heery DM, Kalkhoven E, Hoare S and Parker MG (1997) A signature motif in transcriptional co-activators mediates binding to nuclear receptors. *Nature* 387:733-736.
- Hu B, Collini M, Unwalla R, Miller C, Singhaus R, Quinet E, Savio D, Halpern A, Basso M, Keith J, Clerin V, Chen L, Resmini C, Liu QY, Feingold I, Huselton C, Azam F, Farnegardh M, Enroth C, Bonn T, Goos-Nilsson A,

MOL #65193

- Wilhelmsson A, Nambi P and Wrobel J (2006) Discovery of phenyl acetic acid substituted quinolines as novel liver X receptor agonists for the treatment of atherosclerosis. *J. Med. Chem.* 49:6151-6154.
- Hultén LM, Lindmark H, Diczfalusy U, Björkhem I, Ottosson M, Liu Y, Bondjers G and Wiklund O (1996) Oxysterols present in atherosclerotic tissue decrease the expression of lipoprotein lipase messenger RNA in human monocyte-derived macrophages. *J. Clin. Invest.* 97:461-468.
- Iannone MA, Simmons CA, Kadwell SH, Svoboda DL, Vanderwall DE, Deng SJ, Consler TG, Shearin J, Gray JG and Pearce KH (2004) Correlation between in vitro peptide binding profiles and cellular activities for estrogen receptor-modulating compounds. *Mol. Endocrinol.* 18:1064-1081.
- Jacobson MS (1987) Cholesterol oxides in Indian ghee: possible cause of unexplained high risk of atherosclerosis in Indian immigrant populations. *Lancet* 2:656-658.
- Janowski BA, Willy PJ, Devi TR, Falck JR and Mangelsdorf DJ (1996) An oxysterol signalling pathway mediated by the nuclear receptor LXR alpha. *Nature* 383:728-731.
- Joseph SB, Castrillo A, Laffitte BA, Mangelsdorf DJ and Tontonoz P (2003) Reciprocal regulation of inflammation and lipid metabolism by liver X receptors. *Nat. Med.* 9:213-219.
- Joseph SB, McKilligin E, Pei L, Watson MA, Collins AR, Laffitte BA, Chen M, Noh G, Goodman J, Hagger GN, Tran J, Tippin TK, Wang X, Lusis AJ, Hsueh WA, Law RE, Collins JL, Willson TM and Tontonoz P (2002) Synthetic LXR ligand inhibits the development of atherosclerosis in mice. *Proc. Natl. Acad. Sci. USA* 99:7604-7609.
- Kömüves LG, Schmuth M, Fowler AJ, Elias PM, Hanley K, Man MQ, Moser AH, Lobaccaro JM, Williams ML, Mangelsdorf DJ and Feingold KR (2002) Oxysterol stimulation of epidermal differentiation is mediated by liver X receptor-beta in murine epidermis. *J. Invest. Dermatol.* 118:25-34.
- Kumar N and Singhal OP (1991) Cholesterol oxides and atherosclerosis: A review. *J. Sci. Food Agric.* 55:497-510.
- Lehmann JM, Kliewer SA, Moore LB, Smith-Oliver TA, Oliver BB, Su JL, Sundseth SS, Winegar DA, Blanchard DE, Spencer TA and Willson TM (1997) Activation of the nuclear receptor LXR by oxysterols defines a new hormone response pathway. *J. Biol. Chem.* 272:3137-3140.
- Leonarduzzi G, Sottero B and Poli G (2002) Oxidized products of cholesterol: dietary and metabolic origin, and proatherosclerotic effects (review). *J. Nutr. Biochem.* 13:700-710.
- Ma L, Khalifa B, Yee YK, Lu J, Memezawa A, Savkur RS, Yamamoto Y, Chintalacharuvu SR, Yamaoka K, Stayrook KR, Bramlett KS, Zeng QQ, Chandrasekhar S, Yu X-P, Linebarger JH, Iturria SJ, Burris TP, Kato S, Chin WW and Nagpal S (2006) Identification and characterization of noncalcemic, tissue-selective, nonsecosteroidal vitamin D receptor modulators. *J. Clin. Invest.* 116:892-904.
- Man MQ, Choi EH, Schmuth M, Crumrine D, Uchida Y, Elias PM, Holleran WM and Feingold KR (2006) Basis for improved permeability barrier

MOL #65193

- homeostasis induced by PPAR and LXR activators: liposensors stimulate lipid synthesis, lamellar body secretion, and post-secretory lipid processing. *J. Invest. Dermatol.* 126:386-392.
- Quinet EM, Savio D, Halpern AR, Chen L, Miller C and Nambi P (2004) Gene-selective modulation by a synthetic oxysterol ligand of the liver X receptor. *J. Lipid Res.* 45:1929-1942.
- Savkur RS, Bramlett KS, Clawson D and Burris TP (2004) Pharmacology of nuclear receptor-coregulator recognition. *Vitam. Horm.* 68:145-183.
- Schultz JR, Tu H, Luk A, Repa JJ, Medina JC, Li L, Scwendner S, Wang S, Thoolen M, Mangelsdorf DJ, Lusting K and Shan B (2000) Role of LXRs in control of lipogenesis. *Genes Dev.* 14:2831-2838.
- Smith L and Johnson BH (1989) Biological activities of oxysterols. *Free Radic. Biol. Med.* 7:285-332.
- Staprans I, Pan XM, Rapp JH and Feingold KR (1998) Oxidized cholesterol in the diet accelerates the development of aortic atherosclerosis in cholesterol-fed rabbits. *Arterioscler. Thromb. Vasc. Biol.* 18:977-983.
- Staprans I, Pan XM, Rapp JH and Feingold KR (2003) Oxidized cholesterol in the diet is a source of oxidized lipoproteins in human serum. *J. Lipid Res.* 44:705-715.
- Staprans I, Pan XM, Rapp JH and Feingold KR (2005) The role of dietary oxidized cholesterol and oxidized fatty acids in the development of atherosclerosis. *Mol. Nutr. Food Res.* 49:1075-1082.
- Staprans I, Pan XM, Rapp JH, Grunfeld C and Feingold KR (2000) Oxidized cholesterol in the diet accelerates the development of atherosclerosis in LDL receptor- and apolipoprotein E-deficient mice. *Arterioscler. Thromb. Vasc. Biol.* 20:708-714.
- Staprans I, Pan XM, Rapp JH, Moser AH and Feingold KR (2006) Ezetimibe inhibits the incorporation of dietary oxidized cholesterol into lipoproteins. *J. Lipid Res.* 47:2575-2580.
- Tontonoz P and Mangelsdorf DJ (2003) Liver X receptor signaling pathways in cardiovascular disease. *Mol. Endocrinol.* 17:985-993.
- Vine DF, Mamo CL, Beilin LJ, Mori TA and Croft KD (1998) Dietary oxysterols are incorporated in plasma triglyceride-rich lipoproteins, increase their susceptibility to oxidation and increase aortic cholesterol concentration of rabbits. *J. Lipid Res.* 39:1995-2004.
- Zelcer N, Khanlou N, Clare R, Jiang Q, Reed-Geaghan EG, Landreth GE, Vinters HV and Tontonoz P (2007) Attenuation of neuroinflammation and Alzheimer's disease pathology by liver x receptors. *Proc. Natl. Acad. Sci. USA* 104:10601-10606.
- Zelcer N and Tontonoz P (2006) Liver X receptors as integrators of metabolic and inflammatory signaling. *J. Clin. Invest.* 116:607-614.
- Zheng Y, Du X, Wang W, Boucher M, Parimoo S and Stenn KS (2005) Organogenesis from dissociated cells: Generation of mature cycling hair follicles from skin-derived cells. *J. Invest. Dermatol.* 124:867-876.

MOL #65193

FOOTNOTES

#TJB and QS contributed equally to the manuscript

*Correspondence should be addressed to S.N. (sunil.nagpal@merck.com)

¹Current address: Leonard P. Freedman,
Professor of Biochemistry and Molecular Biology
Jefferson Medical College
Thomas Jefferson University
1025 Walnut St. College 100
Philadelphia, PA 19107

²Current address: Sunil Nagpal,
Respiratory & Immunology
Merck Research Laboratories
770 Sumneytown Pike, West Point, PA 19846-0004

MOL #65193

FIGURE LEGENDS

Figure 1. Chemical structures of $5\alpha,6\alpha$ -epoxycholesterol (5,6-EC), 24,25-epoxycholesterol (24,25-EC), 22-hydroxycholesterol (22-OHC) and 25-hydroxycholesterol (25-OHC).

Figure 2. Characterization of $5\alpha,6\alpha$ -EC and known LXR ligands in the multiplexed cofactor interaction assay.

The interactions of purified 10nM GST-tagged LXR α (A) or LXR β (B) LBDs with 39 cofactor peptides were analyzed in a multiplexed assay using Luminex beads. The LXR LBDs were incubated with the cofactor peptide beads, as listed in Table 1, along with 10 μ M ligand for 2 hrs at room temperature. The data is represented as the mean fluorescence intensity (MFI) in the presence of each ligand, subtracting the background mean fluorescence intensity produced in the presence of DMSO vehicle alone.

Figure 3. Dose response analysis of LXR ligands using pair-wise LXR / cofactor interaction assays.

The interaction of purified 5nM GST-tagged LXR α (A,C) or LXR β (B,D) LBDs with 5nM of the coactivator peptides SRC-2 III (A,B) or SRC-3 III (C,D) were measured using AlphaScreen beads. The LXR LBDs were incubated with cofactor peptides, AlphaScreen beads and serial dilutions of ligands for 2 hrs. The data were fit to a four-parameter nonlinear logistic model to determine the EC_{50s} for each compound. The efficacy was calculated as a percentage of the maximal activity induced by T0901317. Dose response curves for T0901317 (diamonds with dark blue lines), 5,6-EC (squares with red lines), 24,25-EC (triangles with green lines), 22-OHC (crosses with light blue

MOL #65193

lines) and 25-OHC (asterisks with grey lines) are shown. The results for each compound are reported in parentheses as ($EC_{50} \pm SE$; efficacy).

Figure 4. Comparison of 5,6-EC and 24,25-EC in a competition LXR binding assay.

Competition by (A) 5,6-EC and (B) 24,25 EC for 5nM 3H-T0901317 binding to biotinylated LXR α and LXR β LBD proteins was measured. IC_{50s} were calculated using a four-parameter nonlinear logistic model. The results are reported in parentheses as ($IC_{50} \pm SE$).

Figure 5. The activity of LXR ligands in a cell-based mammalian two-hybrid assay.

To assess the activity of LXR ligands in cells, COS-7 cells were co-transfected with GAL4-LXR LBD, VP16-SRC-2, and a 5x-GALUAS luciferase reporter. The dose-response curves for the ligands with LXR α (A) and LXR β (B) are shown. The data were fit to a four-parameter nonlinear logistic model to determine the EC_{50s} for each compound. The efficacy was calculated as a percentage of the maximal activity induced by T0901317. Dose response curves for T0901317 (diamonds with dark blue lines), 5,6-EC (squares with red lines), 24,25-EC (triangles with green lines), 22-OHC (crosses with light blue lines) and 25-OHC (asterisks with grey lines) are shown. The results for each compound are reported in parentheses as ($EC_{50} \pm SE$; efficacy).

Figure 6. 5,6-EC antagonizes 24,25-EC induced Abca1 and Ivl expression in wild type primary murine keratinocytes.

Primary keratinocytes were isolated from wild type or LXR β KO new born mice skin. Cells were treated for 24 hours with vehicle (open bars), 5,6EC (10 μ M; grey bars), 24,25-EC (10 μ M; hatched bars) or co-treated with 5,6-EC and 24,25-EC (10 μ M each;

MOL #65193

black bars). The relative expression level of *Abca1* (A) and *Ivl* (B) was measured by real time PCR.

Figure 7. Effects of 5,6-EC and other ligands on the expression of LXR-responsive genes in primary murine keratinocytes.

Primary keratinocytes were isolated from wild type (WT) or LXR β KO new born mice skin. Cells were treated for 24 hours with vehicle (open bars), 5,6-EC (10 μ M; light grey bars), T0901317 (1 μ M; hatched bars), 5,6-EC + T0901317 (5,6-EC 10 μ M and T0901317 1 μ M; dark gray bars), 24,25-EC (10 μ M; striped bars) or 5,6-EC + 24,25-EC (10 μ M each; black bars). The relative expression level of *Apoe* (A), *Scd1* (B) and *Cyp27a1* (C) was measured by real time PCR.

Figure 8. Antagonism of LXR-mediated gene expression by 5,6-EC in Huh-7 cells.

Huh-7 cells were treated with LXR ligands (5,6-EC at 10 μ M and T0901317 at 1 μ M) for 24 hours as indicated in the figure. The relative expression level of *FASN* (A), *SREBF1* (B), *SLC2A4* (C), *PLTP* (D), *ACACA* (E) and *LDLR* (F) was measured by real time PCR.

Figure 9. Antagonism of LXR-mediated gene expression by 5,6-EC in A549 cells.

A549 cells were treated with LXR ligands (5,6-EC at 10 μ M and T0901317 at 1 μ M) for 24 hours as indicated in the figure. The relative expression level of *ABCA1* (A), *ABCG1* (B), *ACACA* (C), *FASN* (D), *SCD1* (E) and *LDLR* (F) was measured by real time PCR.

Figure 10. 5,6-EC is a partial agonist of *ABCA1* expression in THP-1 macrophages.

Differentiated THP-1 macrophages were treated with varying concentrations of T0901317 (circles), 24,25-EC (squares) or 5,6-EC (triangles) for 18 hours. Percentage expression of *ABCA1* obtained by the three LXR ligands relative to that obtained by

MOL #65193

T0901317 (10 μ M) is shown in the figure (A). Differentiated THP-1 macrophages were treated with vehicle (V), T0901317 (45 nM) or T0901317 (45 nM) + 5,6-EC (30 μ M). The expression of ABCA1 is presented as fold-change (relative to vehicle treatment) in the figure (B). ABCA1 expression was measured by real time PCR.

MOL #65193

Table 1. Biotinylated Cofactor Peptides

Bead #	Peptide	RefSeq #	N-biotin peptide sequences
1	SRC-1 I	NP_003734	KKDSKYSQTSHKLVQLLTTTAEQQR
2	SRC-1 II	NP_003734	HSSLTERHKILHRLLEGGSPSDITT
3	SRC-1 III	NP_003734	KKKESKDHQLLRYLLDKDEKDLRST
4	SRC-1 IV	NP_003734	TQKPTSGPQTPQAQQKSLQQLLTE
5	SRC-2 I	NP_006531	RLHDSKGGTKLLQLLTTKSDQMEPS
6	SRC-2 II	NP_006531	GTSLKEKHKILHRLLDSSSPVDLA
7	SRC-2 III	NP_006531	VSPKKKENALLRYLLDKDDTKDIGL
8	SRC-3 I	NP_858045	GPLESKGHKLLQLLTCSSDDRHS
9	SRC-3 II	NP_858045	GSLLEKHRILHKLLQNGNSPAEVA
10	SRC-3 III	NP_858045	SPKKKENALLRYLLDRDDPSDALS
11	DRIP205 I	NP_004765	KKDFSQVSNPILTSLLQITGNGG
12	DRIP205 II	NP_004765	MAGNTKNHPMLMNLKDNPAQDFST
13	PGC-1a	NP_037393	PPQEAEEPSLLKLLAPANTQLSY
14	PGC-1b I	NP_573570	KKPAPEVDELSLLQKLLATSYP
15	PGC-1b II	NP_573570	KKSKASWAEFSILRELLAQDVLCDVSK
16	CBP I	NP_004371	VPDAASKHKQLSELLRGGSGSSINP
17	CBP/p300 II	NP_004371	PEKRKLIQQQLVLLHAHKCQRREQ
18	CBP III	NP_004371	QPPRSISPSALQDLLRTLKSPSSPQ
19	p300 I	NP_001420	VQDAASKHKQLSELLRSGSSPNLNM
20	p300 II	NP_001420	LKPGTVSQQALQNLRLTLRSPSSPL
21	PCAF	NP_003875	DADTKQVYFYLFKLLRKSILQRGKP
22	NCOR1 I	NP_006302	KKGKTTITAAANFIDVIITRQIASDK
23	NCOR1 II	NP_006302	KKTHRLITLADHICQIITQDFARN
24	NCOR1 III	NP_006302	KKSFADPASNLGLEDIIRKALMGS
25	SMRT I	NP_006303	HQRVVTLAQHISEVITQDYTRHHPQ
26	SMRT II	NP_006303	VQEHASTNMGLEAIIRKALMGKYDQ
27	NRIP1 I	NP_003480	VHQDSIVLTYLEGLLMHQAAGGSGTKK
28	NRIP1 II	NP_003480	VPKGKQDSTLLASLLQSFSSRLQTV
29	NRIP1 III	NP_003480	LRCYGVASSHLKTLKKSKVKDQKP
30	NRIP1 IV	NP_003480	SPKPSVACSQLALLSSEAHLLQQYSKK
31	NRIP1 V	NP_003480	NIKQAANNSLLLHLLKSQTIPKPMN
32	NRIP1 VI	NP_003480	SKLNSHQKVTLLQLLLGHKNEENVE
33	NRIP1 VII	NP_003480	IENLLERRTVLQLLGNPNKGKSEK
34	NRIP1 VIII	NP_003480	QDFSFSKNGLLSRLLRQNQDSYLAD
35	NRIP1 IX	NP_003480	WARESKSFNVLKQLLSENCVRDLS
36	ARA70 I	NP_005428	EETLQQQAQQLYSLLGQFNCLTHQLKK
37	ARA70 II	NP_005428	ENGSRSEKFKLLFQSYNVNDWL
38	MNAR I	NP_055204	PATMELAVAVLRDLLRYAAQLPALFKK
39	MNAR II	NP_055204	ALFRDISMNHLPGLLTSLLGLRPEC
40	Biotin	Control	

TABLE LEGEND

MOL #65193

Table 1. Sequence of nuclear receptor cofactor peptides used in the multiplex assay.

This table lists the sequences and the NCBI reference sequence (RefSeq) accession numbers of the 39 peptides used in the multiplexed cofactor assay.

Fig. 1

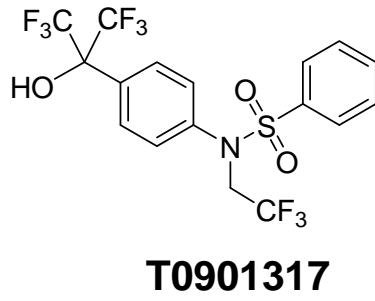
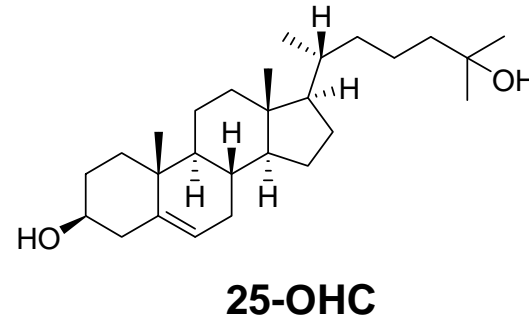
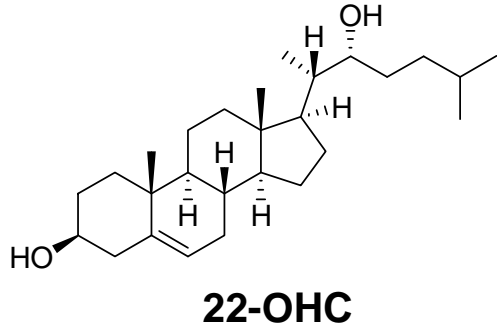
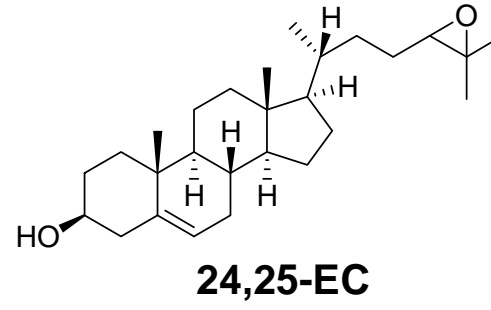
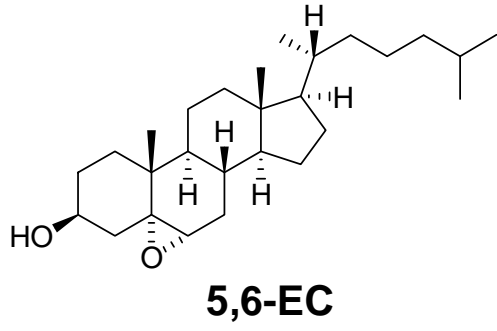


Fig. 2

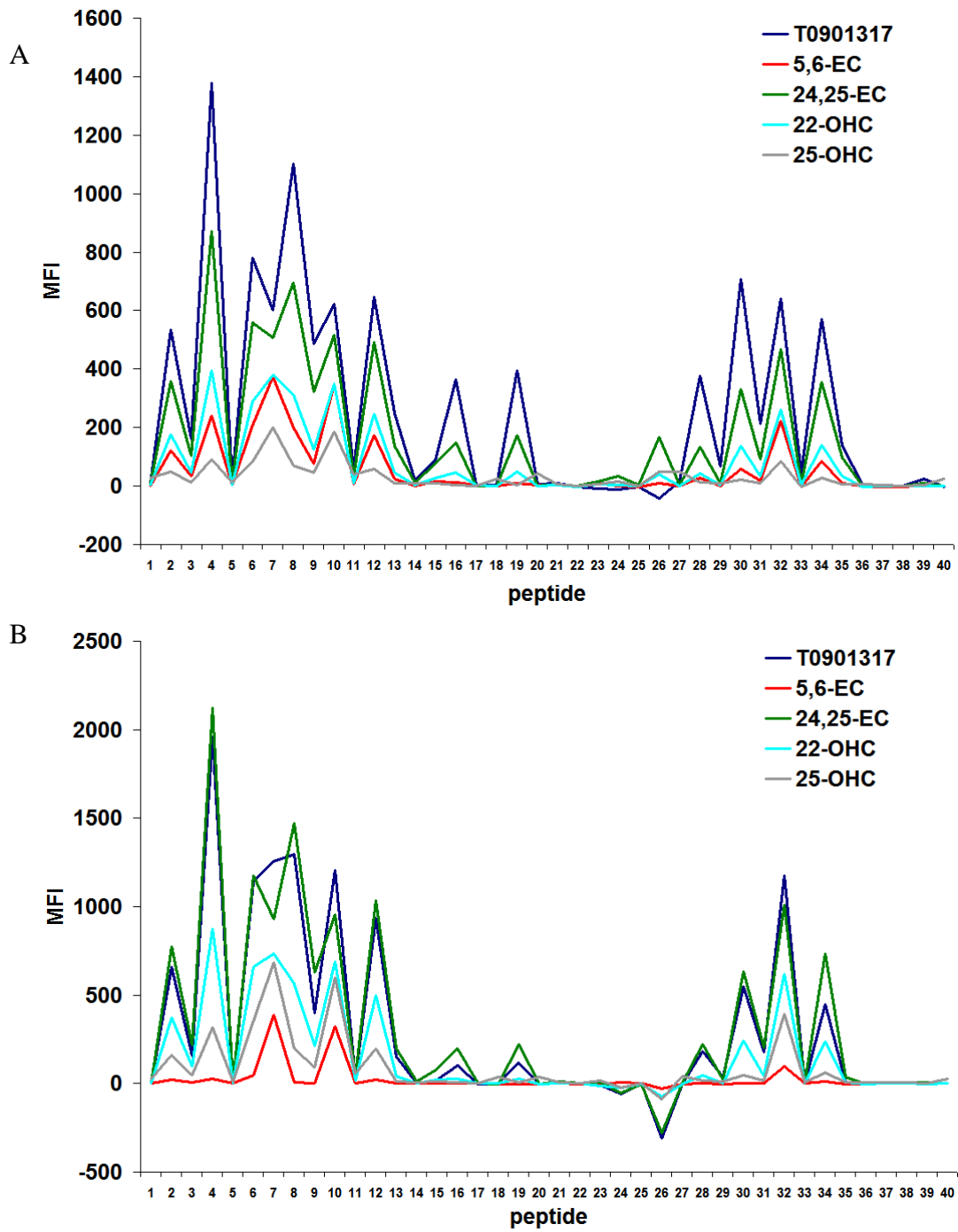
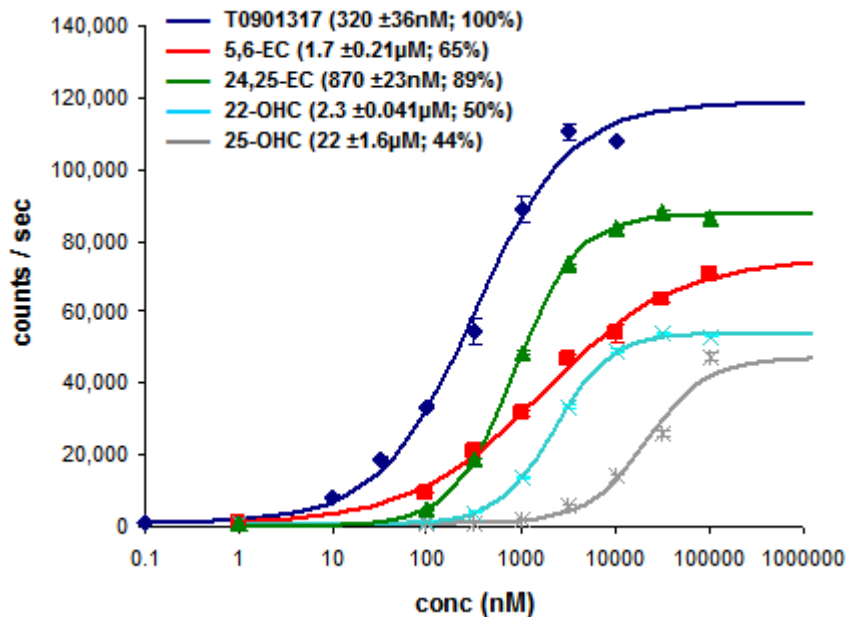
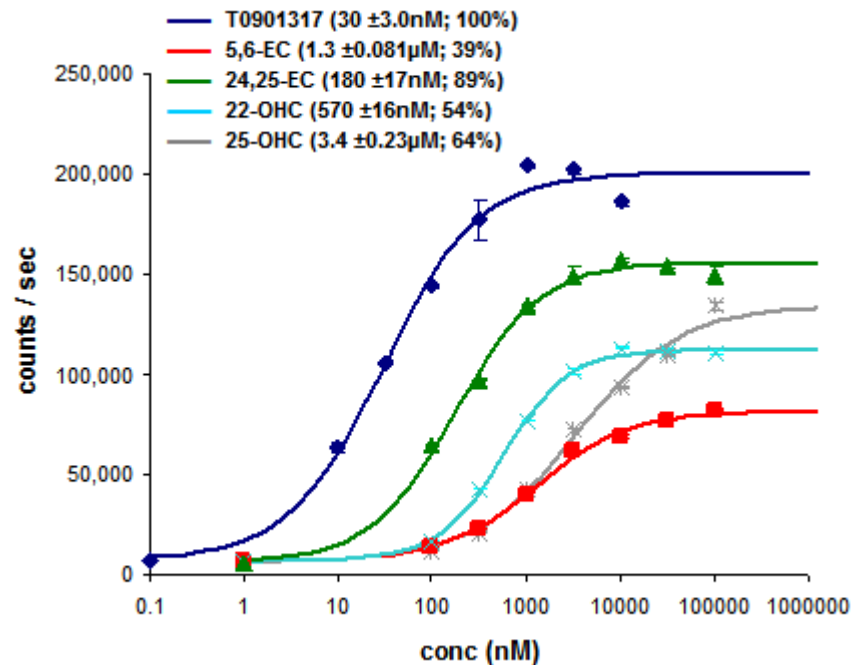


Fig. 3

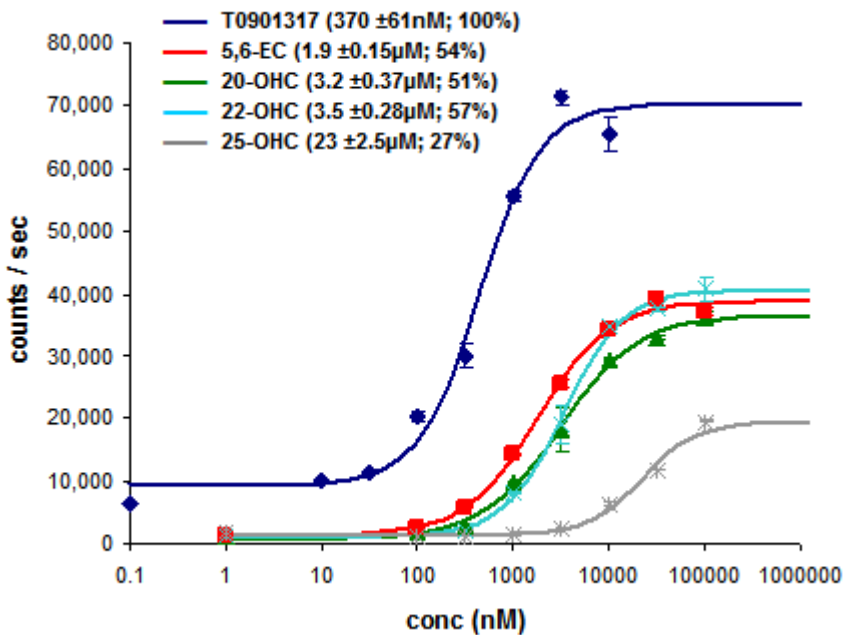
A



B



C



D

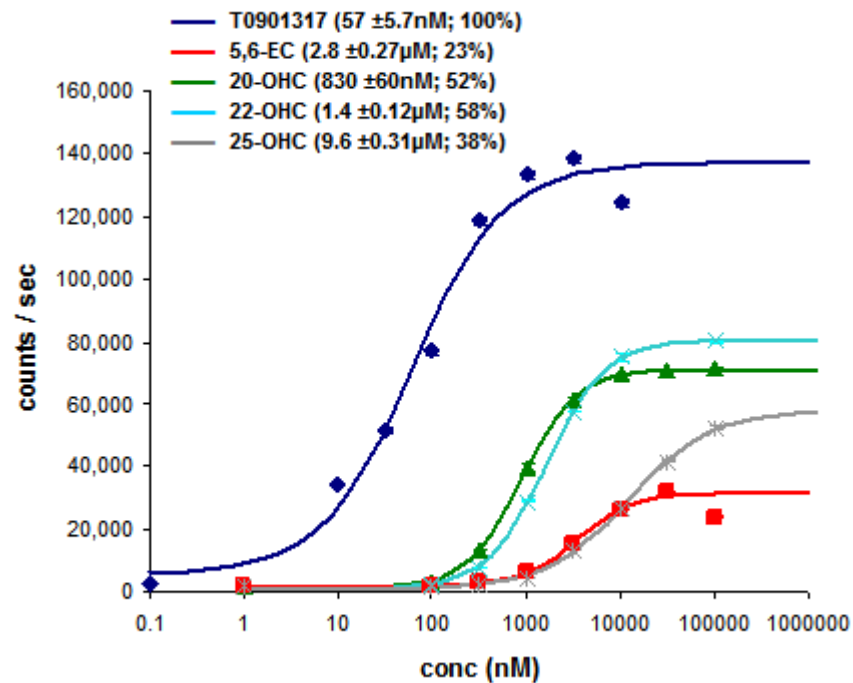
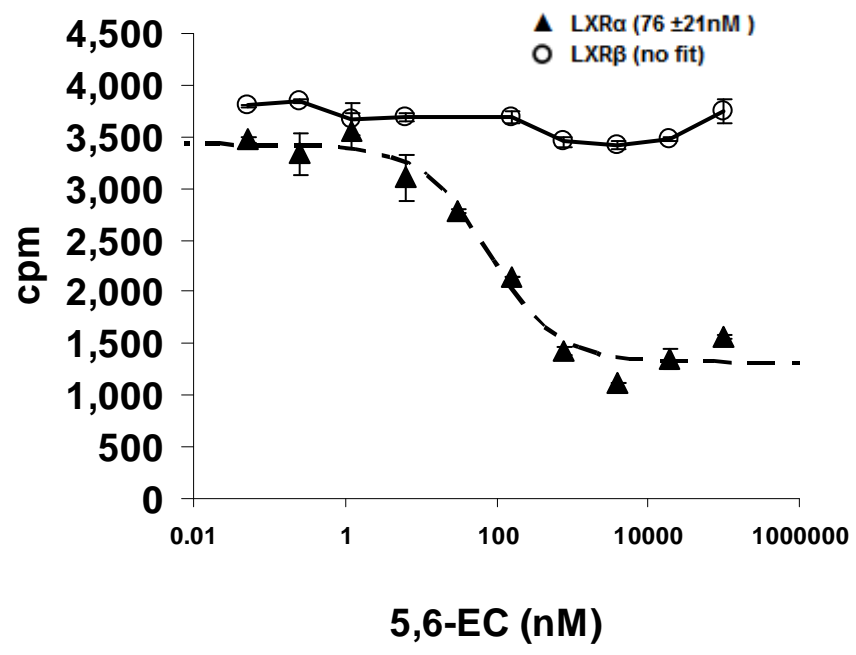


Fig. 4

A



B

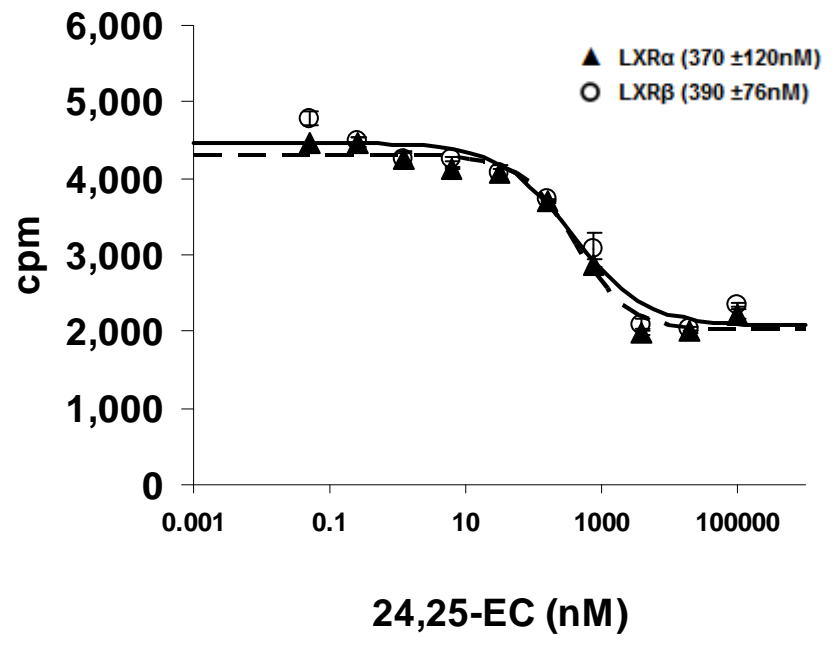


Fig. 5

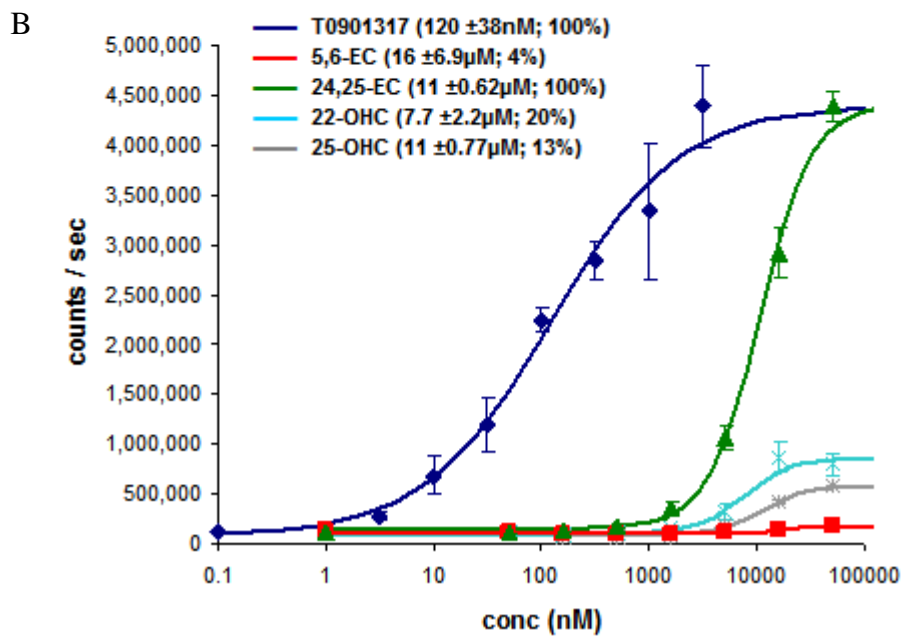
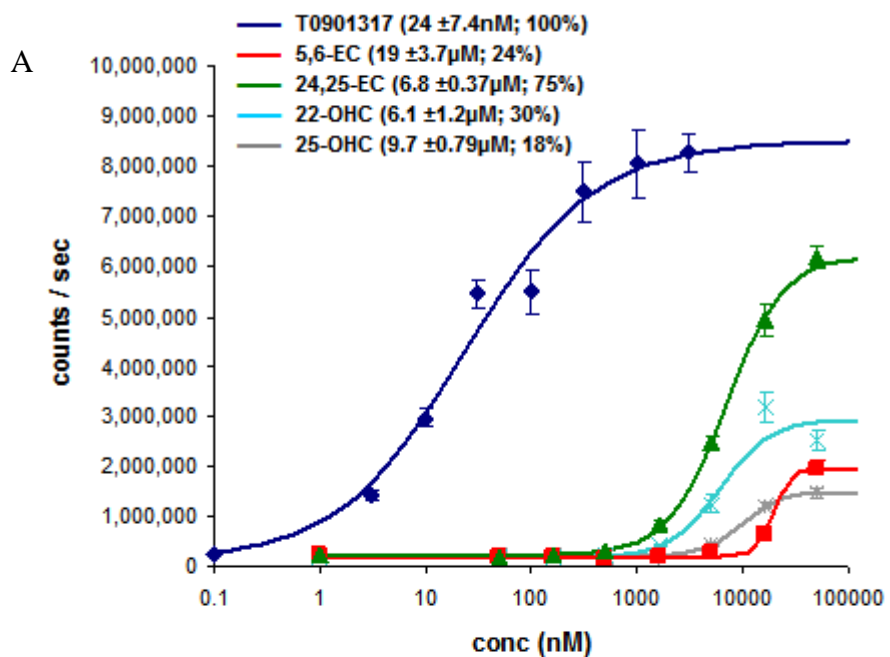


Fig. 6

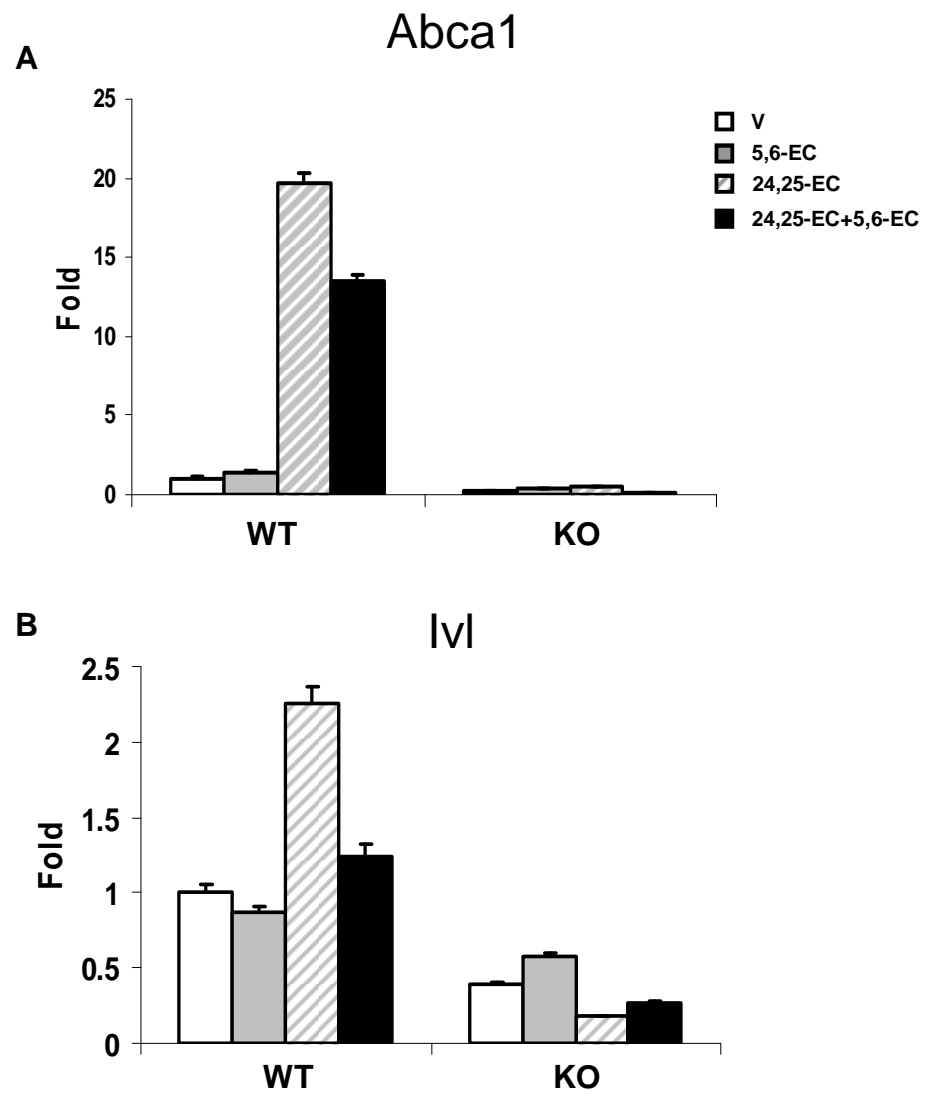


Fig. 7

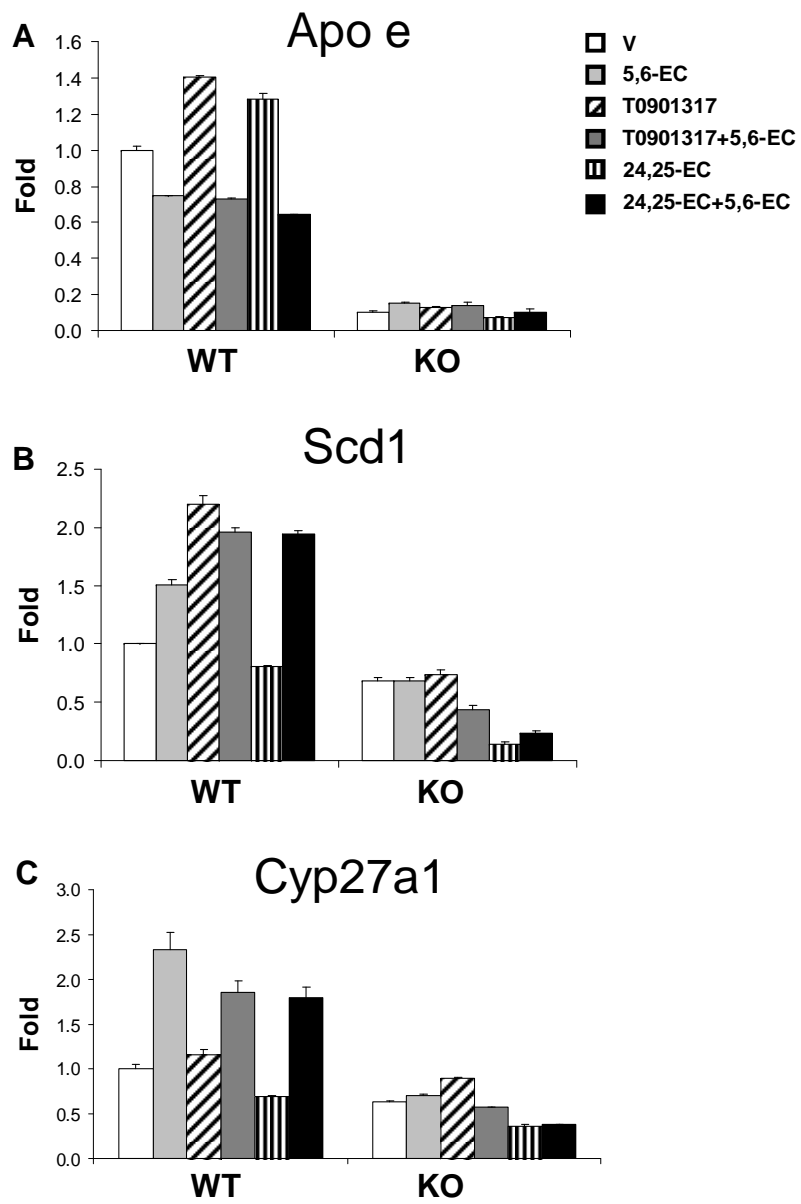


Fig. 8

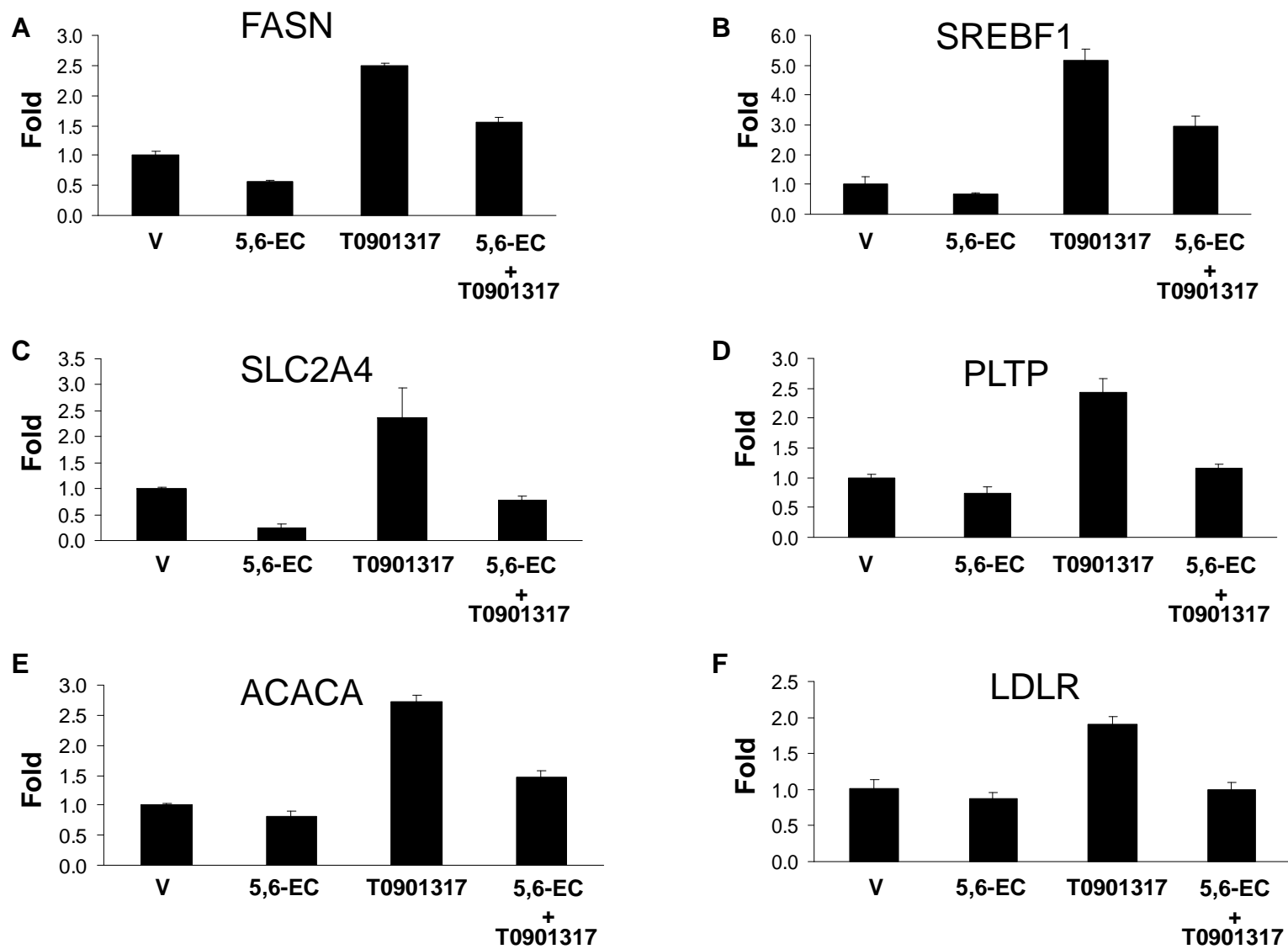


Fig. 9

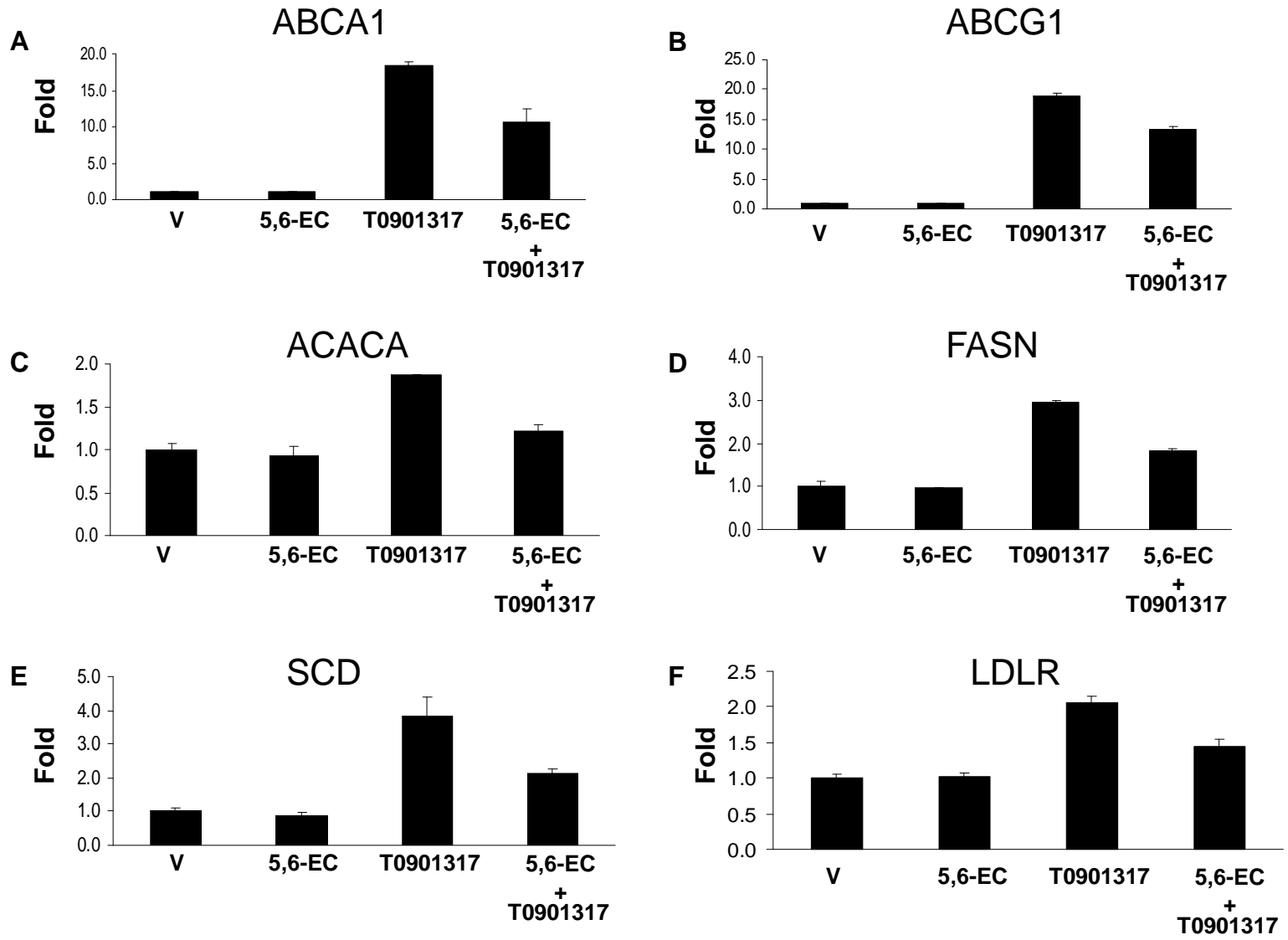


Fig. 10

